# Electron Trajectories in a Field Emission Microscope*

ALLAN M. RUSSELL
*Department of Physics, University of California, Riverside, California*
(Received September 22, 1961)

Trajectories of electrons in a field emission microscope have been calculated for the case of a tip and screen taken as confocal hyperboloids of revolution. The calculations were done in prolate spheroidal coordinates by an iterative method utilizing Hamilton's equations. An IBM digital computer has been programmed to accept values for the initial position and momentum of the electron, the tip and screen radii (each measured at the apex), the tip-to-screen distance and the applied voltage. A calculation yields the final values of position and momentum components at the screen as well as the transit time for the electron. The results of the calculation have been used to predict a field emission pattern which is compared with an experimental pattern. Good agreement is obtained without the use of any adjustable parameters.

## INTRODUCTION

THE field emission microscope, introduced in its present form by Müller[1] in 1937, is shown schematically in Fig. 1. Its essential components are the emitter, a needle-like metal tip with a radius of curvature at the apex of from $10^{-6}$ to $10^{-4}$ cm, and an anode-screen in the form of a phosphor-covered conducting coating on a glass envelope. Application of a potential difference of the order of several thousand volts between the emitter and the anode will create a large electric field at the emitter tip. When the emitter is negative with respect to the anode-screen the potential barrier for electrons at the surface of the metal becomes sufficiently thin that electrons can tunnel through the metal surface. Such electrons become free electrons in the electric field between the emitter tip and the screen. These electrons cause the formation of patterns on the screen which depend upon the crystallographic orientation of the tip and the variation in work function and electric field on its surface. Details of the design and operation of a field emission microscope may be found in recent review articles.[2–4]

Most of the theory of operation developed thus far deals with the theory of field emission *per se* and the interdependence of current, voltage, electric field and tip geometry found in a field emission microscope. Several calculations of the limit of resolution of the microscope have been made.[5–7] In particular, Rose[8] computed the paraxial trajectories expected for electrons very near the apex of a paraboloidal tip in order to determine the resolution.

Both the crystallographic projection of the tip onto the screen and the resolution of the microscope depend upon the trajectories of the electrons. This paper describes a calculation of the trajectories of electrons emitted from a tip for the case when the emitter and the anode screen may be considered confocal hyperboloids of revolution.

## CALCULATION OF TRAJECTORIES

### Shape of the Emitter

Calculations of the electric field strength at the tip have been made for several emitter geometries. Müller[9] and Haefer[10] approximated the tip geometry with an hyperboloid of revolution. Becker[11] and Rose[8] used a paraboloid of revolution. A combination of a sphere mounted on an orthogonal cone was used as the core for a calculation of an equipotential surface as a model of a tip by Dyke and co-workers[12] and much success was achieved by Dreschler and Henkel[13] through the combination of a sphere and an hyperboloid.

Of the geometric forms mentioned the two which are best suited to calculations of the detailed trajectories of the electrons in the microscope are the hyperboloid and

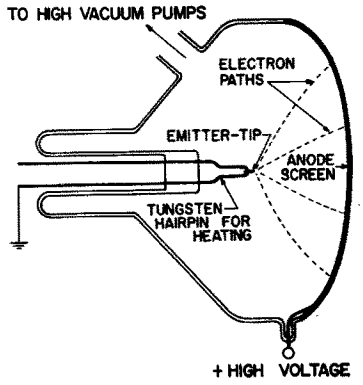


FIG. 1. Diagram of a field emission microscope.

* Supported, in part, by the Office of Naval Research and the Research Corporation.

[1] E. W. Müller, Z. Physik **106**, 132 (1937).
[2] R. H. Good and E. W. Müller, *Handbuch der Physik* (Springer-Verlag, Berlin, 1956), Vol. XXI, pp. 176–231.
[3] W. P. Dyke and W. W. Dolan, *Advances in Electronics* (Academic Press Inc., New York, 1956), Vol. VIII.
[4] R. Gomer, *Field Emission and Field Ionization* (Harvard University Press, Cambridge, Massachusetts, 1961).
[5] E. W. Müller, Z. Physik **120**, 270 (1943).
[6] F. Ashworth, *Advances in Electronics* (Academic Press Inc., New York, 1951), Vol. III, p. 1.
[7] R. Gomer, J. Chem. Phys. **20**, 1772 (1952).
[8] D. J. Rose, J. Appl. Phys. **27**, 215 (1956).
[9] E. W. Müller, Z. Physik **108**, 668 (1938).
[10] R. Haefer, Z. Physik **116**, 604 (1940).
[11] J. A. Becker, Bell System Tech. J. **30**, 907 (1951).
[12] W. P. Dyke, J. K. Trolan, W. W. Dolan, and G. Barnes, J. Appl. Phys. **24**, 570 (1953).
[13] M. Drechsler and E. Henkel, Z. angew. Phys. **6**, 341 (1954).

the paraboloid. The former will be the subject of the calculations described here.

### The Coordinate System

The calculations are most easily carried out in an orthogonal coordinate system where both the emitter and the anode screen may be represented as equipotential surfaces formed by setting one of the coordinate variables equal to a constant. Prolate spheroidal coordinates satisfy this requirement. Figure 2 shows the coordinate system in two dimensions, $\eta$ and $\xi$, and its relationship to cartesian coordinates. The third dimension $\phi$ is obtained by rotating the figure about the $Z'$ coordinate axis. The equations for the transformation from cartesian coordinates to prolate spheroidal coordinates and their converse are given in Appendix I.

The emitter surface may now be chosen as an hyperboloid $\eta=\eta_e$ with apex very near the focus. Choice of the particular hyperboloid will depend upon the radius of curvature $R_e$ of the emitter apex. The anode screen radius $R_s$ and the tip to screen distance $d$ determine the choice of $\eta_s$ and of the interfocal distance $2a$ of the coordinate system to be used.

Combining the equation for the radius of curvature at the apex of a hyperboloid with the equation for the distance of the apex from the focus yields,

$$a=d(R_s-d)/(R_s-2d).$$

It should be noted that, because of limitations on the values of $\eta_s$, a solution to this equation can be found only for those cases when the radius of curvature of the screen exceeds twice the distance from the tip to the screen.

Surfaces of constant $\eta$ represent equipotential surfaces and lines of constant $\xi$ and $\phi$ represent the electric field lines. It is now possible to derive the equations of motion of an electron moving in the electric field of the microscope.

### Equations of Motion

The kinetic energy of an electron of mass $m$ is

$$T=\tfrac{1}{2}mv^2=\tfrac{1}{2}m(\dot{X}'^2+\dot{Y}'^2+\dot{Z}'^2). \tag{1}$$

In prolate spheroidal coordinates this becomes,

$$T=\frac{a^2m}{2}\left[\frac{(\xi^2-\eta^2)}{(\xi^2-1)}\dot{\xi}^2+\frac{(\xi^2-\eta^2)}{(1-\eta^2)}\dot{\eta}^2+(\xi^2-1)(1-\eta^2)\dot{\phi}^2\right], \tag{2}$$

where $a$ is the distance from the focus to the origin in cartesian coordinates.

The potential energy $V$ may be obtained from Laplace's equation in prolate spheroidal coordinates as follows,

$$\nabla^2\psi=\frac{1}{a^2(\xi^2-\eta^2)}\left[\frac{\partial}{\partial\eta}(1-\eta^2)\frac{\partial\psi}{\partial\eta}\right]=0. \tag{3}$$

Integration of the above expression yields

$$(1-\eta^2)\frac{\partial\psi}{\partial\eta}=A, \quad \text{or} \quad \frac{\partial\psi}{\partial\eta}=\frac{A}{1-\eta^2},$$

where $A$ is a constant of integration. The equation for $\psi$ may be obtained by integrating the last expression.

$$\psi=\frac{A}{2}\ln\frac{1+\eta}{1-\eta}+B. \tag{4}$$

The application of boundary conditions permits the evaluation of $A$ and $B$. If the potential of the screen is zero then $\psi=0$ when $\eta=\eta_s$, and

$$B=-\frac{A}{2}\ln\frac{1+\eta_s}{1-\eta_s}.$$

If the potential of the emitter is $-V_0$, then $\psi=-V_0$ when $\eta=\eta_e$, and

$$A=-\frac{2V_0}{\ln\left[\frac{1-\eta_s}{1+\eta_s}\cdot\frac{1+\eta_e}{1-\eta_e}\right]},$$

therefore the potential energy may be written,

$$V(\eta)=\frac{eV_0}{\ln\left[\frac{1-\eta_s}{1+\eta_s}\cdot\frac{1+\eta_e}{1-\eta_e}\right]}\left(\ln\frac{1+\eta}{1-\eta}-\ln\frac{1+\eta_s}{1-\eta_s}\right), \tag{5}$$

when a positive number is used for the charge on the electron.

The conjugate momenta are now calculated by differentiating the Lagrangian, $L=T-V$, with respect to the velocities $\dot{\eta}$, $\dot{\xi}$, and $\dot{\phi}$. When this has been done the

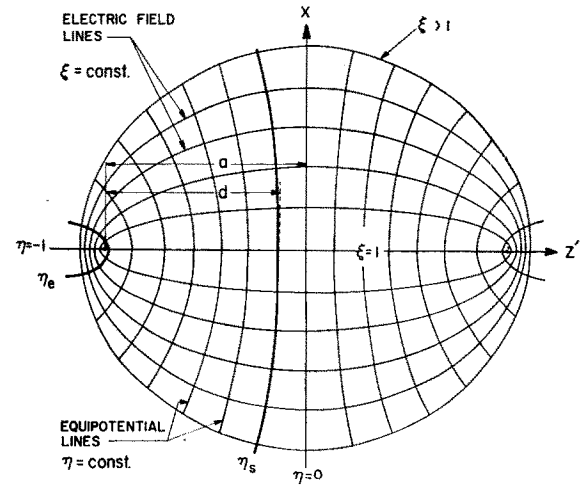


FIG. 2. Prolate spheroidal coordinates showing choices of $\eta_e$ (exaggerated) for the emitter and $\eta_s$ for the screen.

Hamiltonian, $H=T+V$, may be written

$$H=\frac{1}{2a^2m}\left[p_\xi^2\frac{\xi^2-1}{\xi^2-\eta^2}+p_\eta^2\frac{1-\eta^2}{\xi^2-\eta^2}+p_\phi^2\frac{1}{(\xi^2-1)(1-\eta^2)}\right]+\frac{eV_0}{\ln\left[\frac{1-\eta_s}{1+\eta_s}\cdot\frac{1+\eta_e}{1-\eta_e}\right]}\left(\ln\frac{1+\eta}{1-\eta}-\ln\frac{1+\eta_s}{1-\eta_s}\right). \quad (6)$$

The equations of motion in the Hamiltonian formulation may now be written by differentiating (6),

$$\dot{\xi}=\frac{\partial H}{\partial p_\xi},\quad \dot{\eta}=\frac{\partial H}{\partial p_\eta},\quad \dot{\phi}=\frac{\partial H}{\partial p_\phi},$$

$$\dot{p}_\xi=-\frac{\partial H}{\partial \xi},\quad \dot{p}_\eta=-\frac{\partial H}{\partial \eta},\quad \dot{p}_\phi=-\frac{\partial H}{\partial \phi}.$$

It is now possible to calculate the trajectories of a free electron in the microscope given its initial values of position and momentum. This is done by calculating successive values of each position and momentum, using an approximation of the form

$$\xi_1\cong\xi_0+\dot{\xi}_0\Delta t,$$

where $\Delta t$ is taken sufficiently small. Before this can be done, however, three difficulties must be removed.

(1) The variables $\xi$ and $\eta$ are very nearly equal to one near the tip and are not sufficiently sensitive.

(2) The initial conditions are more easily specified in cartesian coordinates.

(3) The final values of position and momentum at the screen are desired in cartesian coordinates.

These problems can be solved by the appropriate coordinate transformations which will now be described.

### Transformation of Coordinates

The first problem has to do with the values of the coordinate variables in the neighborhood of the tip. The difficulty becomes apparent when the radius of curvature of the apex of the emitter $R_e$ is expressed in terms of $\eta_e$.

$$R_e=-(a/\eta_e)(1-\eta_e^2). \quad (7)$$

Because $R_e$ is of the order of $10^{-5}$ cm and $a$ is of the order of 10 cm, $\eta_e$ has a value very nearly equal to $-1$. This means that many significant figures must be retained in the calculation if an accurate result is to be expected since most of the acceleration of the electron takes place in the region of very high electric field near the surface of the emitter. Furthermore, since the electron is nearly on the $Z'$ axis when it leaves the tip the value of $\xi$ is also nearly one and the same difficulty exists in this coordinate.

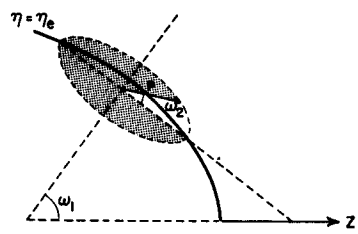


FIG. 3. An electron at the surface of the tip showing the relationship between initial position and momentum.

To avoid these problems the following transformations can be made

$$\alpha=\eta+1,\quad \beta=\xi-1,\quad \text{and}\quad \gamma=\phi. \quad (8)$$

The values of $\alpha$ and $\beta$ near the surface of the emitter will now be approximately zero and the value of $\alpha$ at the screen will be nearly 1. The equations of motion which result from the transformations (8) are given in Appendix I.

The transformation from cartesian coordinates to prolate spheroidal coordinates at the tip is facilitated by the fact that near the tip $\alpha\ll1$ and $\beta\ll1$. At the same time it is convenient to transform the cartesian coordinates so that the origin coincides with the focus of the hyperboloids being used rather than with the plane. This is accomplished with the following transformations,

$$X=X',\quad Y=Y',\quad \text{and}\quad Z=Z'+a. \quad (9)$$

The approximate transformations near the tip from these new cartesian coordinates to prolate spheroidal coordinates are given in Appendix I.

The last set of transformations required are those needed to go from prolate spheroidal coordinates to cartesian coordinates near the anode screen. Fortunately these equations are exact as no approximations were necessary. These equations are also listed in Appendix I.

The initial values of position and momentum are specified in terms of tip radius, the angle $\omega_1$, made by the normal to the surface of the tip and the tip axis, the initial momentum tangent to the tip surface and the angle $\omega_2$ between the momentum vector and a tangent line in the plane which includes the tip axis. This is most easiiy seen by referring to Fig. 3.

The final position of the electron on the screen is specified by values of $X$ and $Y$ as this corresponds to the projection which is achieved when the anode screen is photographed.

### Calculation

The calculation of the trajectories was done on an IBM 1620 digital computer. Values of tip radius, tip-to-screen distance, screen radius, and tip voltage were supplied to the computer as well as the initial values of position and momentum.

Successive values for the position and momenta were

calculated by using the approximations

$$\alpha_{i+1}=\alpha_i+\dot{\alpha}_i\Delta t$$
$$\beta_{i+}=\beta_i+\dot{\beta}_i\Delta t$$
$$\gamma_{i+1}=\gamma_i+\dot{\gamma}_i\Delta t$$
$$p_{\alpha_{i+1}}=p_{\alpha_i}+\dot{p}_{\alpha_i}\Delta t$$
$$p_{\beta_{i+1}}=p_{\beta_i}+\dot{p}_{\beta_i}\Delta t,$$

and the fact that

$$p_\gamma=\text{const.}$$

The calculation was begun with an initial value of $\Delta t$ equal $10^{-16}$ sec. The calculation of successive values of position and momentum was initially repeated with increasingly large values of $\Delta t$. This was continued until the electron passed the screen position. An interpolation was then made and the computer printed out the final values of $X$, $Y$, and $Z$.

Repetition of the calculations with smaller initial values of $\Delta t$ and comparison with final values of momenta with final kinetic energy at the screen indicated sufficient stability in the results that the final values obtained from the calculation could be considered accurate to about 1 percent.

## RESULTS

An experimental tube was constructed which was designed to conform as closely as possible to a theoretical equipotential surface. A tungsten tip was installed in this tube and field emission patterns were obtained. After the tube had been dismantled the tube parameters were found to be

| | |
|---|---|
| Radius of curvature of the screen | 14 cm |
| Radius of curvature of the tip | 5000 A |
| Applied voltage | 5000 volts |
| Tip-to-screen distance | 3.74±0.05 cm. |

Of these parameters only the last is required with appreciable accuracy as the calculation is relatively insensitive to the first three.

These four experimental values satisfied the need for four parameters in the calculation leaving nothing to be adjusted.

Figure 4 shows the results of a calculation using the parameters given above. These results are compared with three experimentally determined points corresponding to the (100) planes and two of the (211) planes.

It can be seen that the agreement between the calculated values and the experimentally determined values deteriorates as the angle with the tip axis is increased. This is due largely to edge effects caused by the finite size of the screen, distortions in the electric field due to the tip supporting loop and deviation of the surface of the tip from the theoretical hyperboloid.

Figure 5 compares the calculated positions corresponding to several of the prominent planes with the experimental pattern. Here again it should be emphasized that the agreement was obtained without adjusting the size either of the calculated pattern or of the experimental pattern. The deviation observed in Fig. 4 is again apparent in the outer (211) planes in Fig. 5.

All the above calculations were carried out for the case of zero initial momentum. Calculations involving the effect of initial momentum tangent to the surface

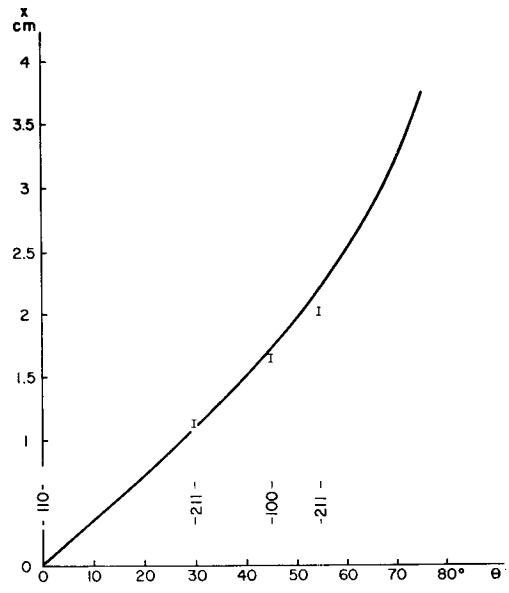


FIG. 4. Final position of electron at the screen as a function of initial angle $\omega_1$ for the case of a tube with tip radius of 5000 A, tip to screen distance 3.74±0.05 cm and screen radius 14 cm. The results is compared with experimental values obtained for three crystallographic planes on 110 orientated tungsten.

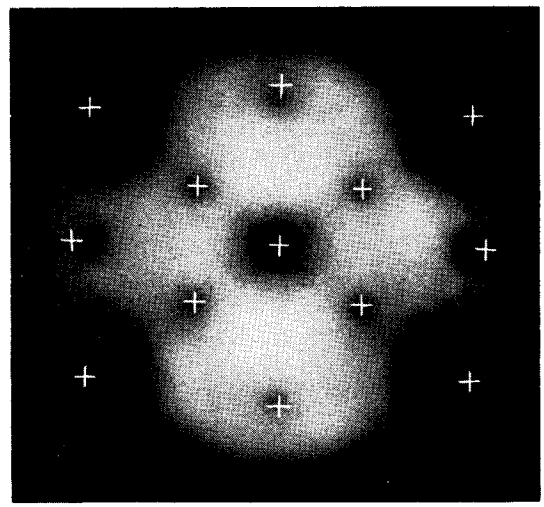

FIG. 5. Field emission pattern from a tungsten tip showing calculated positions corresponding to the (100), (110), and (211) crystallographic planes.

of the tip are being carried out but the results are not complete at this time.

## CONCLUSION

Calculations of electron trajectories in a field emission microscope can be carried out for the case in which the emitter and the screen may be considered to be confocal hyperboloids of revolution. The calculated pattern gives quantitative agreement with the experimental pattern when the experimental tube parameters are used. The agreement is obtained without the use of any adjustable parameters.

## ACKNOWLEDGMENTS

The author would like to thank Professor T. T. Taylor for several important suggestions regarding the calculation and Mr. John Nickel and Mr. Conrad Miziumski for their assistance in the calculations. Thanks also are due Miss Nora Josephson, Mr. Michael Nieto, and Mr. Kenneth Aring for assisting with the experimental measurements.

Finally the author wishes to thank Dr. Morris Garber of the Biometrical Laboratory of the Citrus Experiment Station, UCR for his assistance with the IBM 1620.

## APPENDIX I

### The Coordinate Transformations and Equations of Motion

Transformations from cartesian coordinates to prolate spheroidal coordinates and their converses:

$$X'=a[(\xi^2-1)(1-\eta^2)]^{\frac{1}{2}}\cos\phi$$
$$Y'=a[(\xi^2-1)(1-\eta^2)]^{\frac{1}{2}}\sin\phi$$
$$Z'=a\xi\eta,$$

where $-1\leq\eta\leq 0$ and $1\leq\xi<\infty$,

and

$$\xi=\frac{r_1+r_2}{2a},\quad \eta=\frac{r_1-r_2}{2a},\quad \phi=\tan^{-1}Y'/X',$$

where

$$r_1=[(Z'+a)^2+X'^2+Y'^2]^{\frac{1}{2}},\quad r_2=[(Z'-a)^2+X'^2+Y'^2]^{\frac{1}{2}},$$

and $r_1$ and $r_2$ are distances from the foci.

Results of the transformation of the equation of motion into the coordinates $\alpha$, $\beta$, and $\gamma$, where $\alpha=\eta+1$, $\beta=\xi-1$, and $\gamma=\phi$:

$$H=\frac{1}{2a^2m}\left[\frac{\beta(\beta+2)p_\beta^2+\alpha(2-\alpha)p_\alpha^2}{\beta(\beta+2)+\alpha(2-\alpha)}+\frac{p_\gamma^2}{\beta(\beta+2)\alpha(2-\alpha)}\right]+\frac{eV_0}{\ln\left[\left(\frac{2-\alpha_s}{\alpha_s}\right)\left(\frac{\alpha_e}{2-\alpha_e}\right)\right]}\left(\ln\frac{\alpha}{2-\alpha}-\ln\frac{\alpha_s}{\alpha-\alpha_s}\right)$$

and

$$\dot\alpha=LAp_\alpha,\quad \beta=LBp_\beta,\quad \dot\gamma=LCp_\gamma,$$

$$\dot p_\alpha=LFA\left(p_\alpha^2-p_\beta^2-\frac{C}{AB}p_\gamma^2\right)-KG,$$

$$\dot p_\beta=LDB\left(p_\alpha^2-p_\beta^2+\frac{C}{AB}p_\gamma^2\right),\quad \dot p_\gamma=0,$$

where

$$B=\frac{\alpha(2-\alpha)}{\beta(\beta+2)+\alpha(2-\alpha)},\qquad A=\frac{\beta(\beta+2)}{\beta(\beta+2)+\alpha(2-\alpha)},$$

$$C=\frac{1}{\beta(\beta+2)+\alpha(2-\alpha)},\qquad D=\frac{\beta+1}{\beta(\beta+2)+\alpha(2-\alpha)},$$

$$F=\frac{\alpha-1}{\beta(\beta+2)+\alpha(2-\alpha)},\qquad G=\frac{2}{\alpha(2-\alpha)},$$

$$K=\frac{eV}{\ln\left[\left(\frac{\alpha_e}{2-\alpha_e}\right)\left(\frac{2-\alpha_s}{\alpha_s}\right)\right]},\text{ and }L=\frac{1}{a^2m}.$$

Transformations used to convert the initial position from cartesian coordinates to approximated prolate spheroidal coordinates (near the tip):

$$\alpha=\frac{1}{2a}[Z+(X^2+Y^2+Z^2)^{\frac{1}{2}}],$$

$$\beta=\frac{1}{2a}[-Z+(X^2+Y^2+Z^2)^{\frac{1}{2}}],$$

and

$$\phi=\tan^{-1}Y/X.$$

Equations used to transform the initial momenta into initial velocities in prolate spheroidal coordinates (near the tip):

$$\dot\alpha=\frac{1}{2am}\left[p_Z+\frac{Xp_X+Yp_Y+Zp_Z}{(X^2+Y^2+Z^2)^{\frac{1}{2}}}\right],$$

$$\beta=\frac{1}{2am}\left[-p_Z+\frac{Xp_X+Yp_Y+Zp_Z}{(X^2+Y^2+Z^2)^{\frac{1}{2}}}\right],$$

and

$$\dot\phi=\frac{1}{m}\left(\frac{Xp_Y-Yp_X}{X^2+Y^2}\right).$$

Momenta in prolate spheroidal coordinates (near the tip):

$$p_\alpha=a^2m\dot\alpha\left(1+\frac{\beta}{\alpha}\right),$$

$$p_\beta=a^2m\beta\left(1+\frac{\alpha}{\beta}\right),$$

and $$p_\phi = a^2 m \dot{\phi} \alpha \beta.$$

Transformations used to convert final values of position and momentum from prolate spheroidal coordinates to cartesian coordinates:

$$X = aM \cos\phi,$$

$$Y = aM \sin\phi,$$

$$Z = a(\alpha-1)(\beta+1)+a,$$

$$p_X = \frac{am}{M} L \cos\phi - amM\dot{\phi} \sin\phi,$$

$$p_Y = \frac{am}{M} L \sin\phi + amM\dot{\phi} \cos\phi,$$

and

$$p_Z = am[\dot{\alpha}(1+\beta)+\dot{\beta}(\alpha-1)],$$

where

$$L = [\dot{\alpha}\beta(\beta+2)(1-\alpha)+\dot{\beta}\alpha(\beta+1)(2-\alpha)],$$

and

$$M = [\beta(\beta+2)\alpha(2-\alpha)]^{\frac{1}{2}}.$$

JOURNAL OF APPLIED PHYSICS VOLUME 33, NUMBER 3 MARCH, 1962

# Growth and Photomicrographical Observation of Argon Crystals*

M. BELTRAMI
*Istituto Nazionale di Fisica Nucleare, Sezione di Milano, Milan, Italy*

(Received August 17, 1961)

Argon crystals are grown with Bridgman's method, and the free surface of the crystal is observed with a microscope in reflected light. In order to observe the crystal at various depths, pumping and sublimation operations are effected until the entire crystal sublimates layer after layer. All the crystals obtained showed many coherent and noncoherent twin boundaries; some of them did not show any grain boundary.

## 1. EXPERIMENTAL

A CONSIDERABLE amount of work has been done in the last few years on solid inert gases and particularly on argon, and a certain attention has been paid to the possibility of growing single crystals. Followell[1] in addition to other investigations has studied the growth of argon crystals from the liquid phase by a modified Bridgman's method; after having removed the argon specimen from contact with the glass mould in which it was grown the thermally etched surface was observed through a microscope in transmitted light. Here we have considered the opportunity of re-examining the possibility of growing single crystals of argon, and observing directly the surface of the crystal with a microscope in reflected light.

The growth method we have used is the same used by Stansfield and Followell[2,3] with slight technical modification. The crystal was grown from the liquid argon, with a solid-liquid interface convex towards the liquid; notwithstanding our attempts, it was not possible to obtain a surface convex towards the liquid in the bottom of the crucible (for the first 3 or 4 mm) and thus only a horizontal surface was obtained. Despite this, if the solidification process stops for about a quarter of an hour when the first 3 or 4 mm of solid have been grown, it is quite possible that the solid sample will be a crystal which does not show grain boundaries in all its length, but only a few coherent and noncoherent twin boundaries. In the solidification of the last part of liquid it was necessary to operate very slowly, in order to avoid the production of snow and dendrites, and to obtain a smooth and reflective surface which can be examined by means of our microscope. Figure 1 shows in detail the crucible-microscope system. We used spectroscopically pure argon; the same results, however, were obtained with 99.99% commercial argon; the crystallization rate was from 1 mm/hr to 5 mm/hr.

## 2. PHOTOMICROGRAPHICAL OBSERVATION

Immediately after the solidification of the last film of liquid, we can notice a white reflecting surface, more or less rich in details. These surface details are the same as those noticed by Stansfield and Followell: straight line segments that are interpreted[4–9] as coherent twin boundaries, discontinuous grain boundaries (Fig. 2) that we have agreed to classify as noncoherent twin boundaries, grain boundaries (Fig. 3), and other irregular details.

As soon as the triple point is reached, and the solidification from the liquid is completed, the details

* Work supported by the Consiglio Nazionale delle Ricerche.

[1] R. F. Followell, Ph.D. thesis, University of Bristol, 1957.

[2] D. Stansfield and R. F. Followell, Suppl. Bull. inst. intern. froid **35**, No. 3, 478 (1955).

[3] D. Stansfield, Phil. Mag. **1**, 934 (1956).

[4] B. Chalmers, Progress Metal Phys. **3**, 293 (1952).

[5] R. Clark and G. B. Craig, Progress Metal Phys. **3**, 11 (1952).

[6] B. Chalmers, R. King, and R. Shuttleworth, Proc. Roy. Soc. (London) **A193**, 465 (1948).

[7] A. J. W. Moore, Acta Met. **8**, 653 (1960).

[8] E. D. Hondros and A. J. W. Moore, Acta Met. **8**, 653 (1960).

[9] J. E. Burke and D. Turnbull, Progress Metal Phys. **3**, 220 (1952).